Supplementary Information for

Catalytic kinetic growth of half-metallic hexagonal boron nitride-graphene lateral heterostructure by transition metal single-atom catalyst on Rh(111)

Yandi Zhu,[a] Weihu Li,[a] Xiaoyan Ren,[a] Lili Zhang,[a] Xingju Zhao*[a,b] and Shunfang Li*[a,b]

[a] Key Laboratory of Material Physics, Ministry of Education, School of Physics, Zhengzhou University, Zhengzhou 450001, China

[b] Institute of Quantum Materials and Physics, Henan Academy of Sciences, Zhengzhou 450046, China

Corresponding Authors
*E-mail: zhaoxingju@zzu.edu.cn; sflizzu@zzu.edu.cn

Table of content:

Fig. S1. Comparison of the E_b of B-C and N-C on Rh(111). We have formulated the equation for calculating the E_b per carbon atom, as follows:

$$E_b = (nE_C + E_{X/Rh(111)} - E_{tot})/n, \tag{1}$$

where n is the number of carbon atoms in the calculations, with the three terms of E_C, $E_{X/Rh(111)}$, and E_{tot}, representing the energies of the optimized carbon single atom in gas phase, B and/or N terminated hBN nanoribbons on Rh(111), and n carbon atoms attached to hBN nanoribbons configurations on Rh(111), respectively.
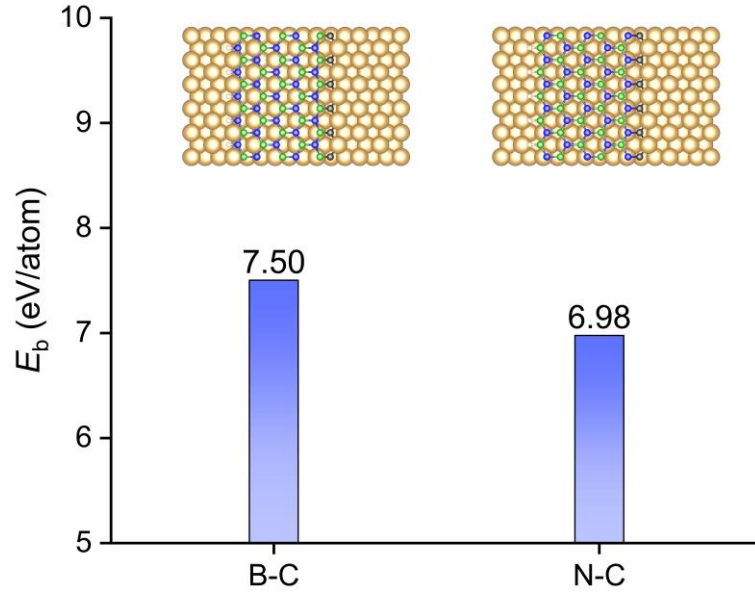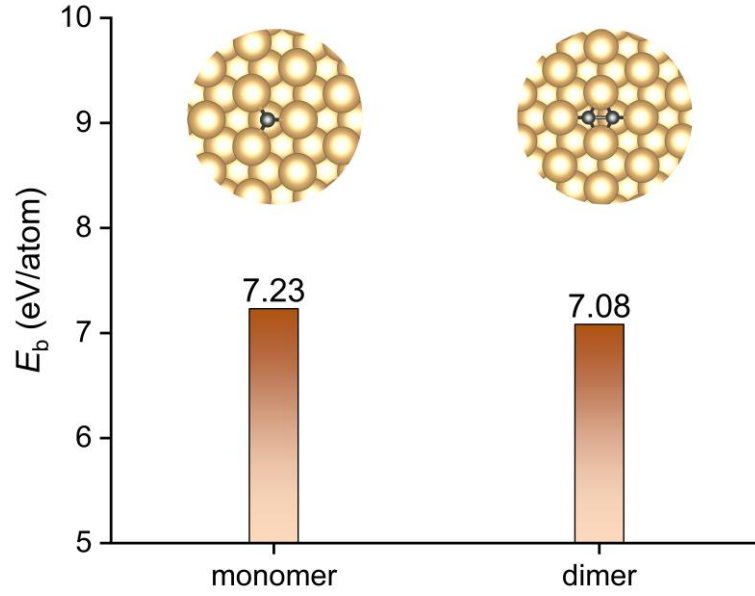
Fig. S2. Comparison of the E_b of carbon monomer and dimer on Rh(111). We have formulated the equation for calculating the E_b per carbon atom, as follows:

$$E_b = (nE_C + E_{Rh(111)} - E_{tot})/n, \qquad (2)$$

where n is the number of carbon atoms in the calculations, with the three terms of E_C, $E_{Rh(111)}$, and E_{tot}, representing the energies of the optimized carbon single atom in gas phase, Rh(111) substrate, and carbon monomer and/or dimer adsorbed to Rh(111) substrate configurations, respectively.
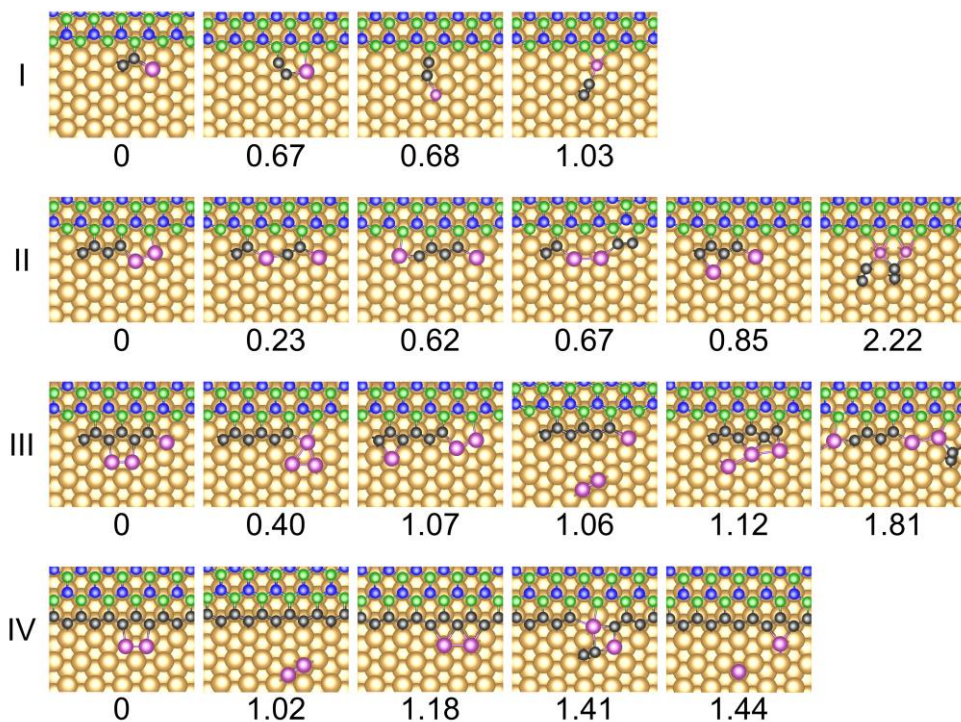
Fig. S3. Configurations and relative energies of the growth of Mo-C$_2$ seeds attaching to the *h*-BN edge on Rh(111).
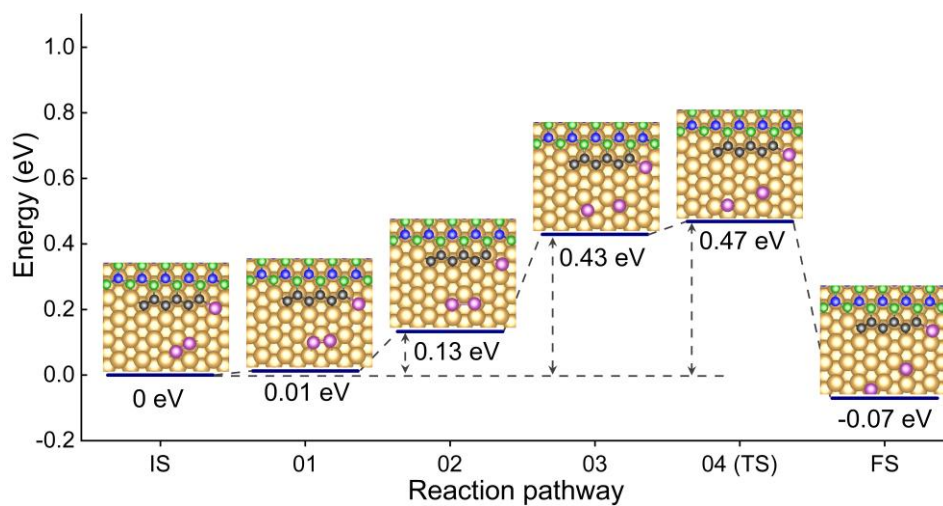
Fig. S4. Reaction pathway and E$_{bar}$ for Mo$_2$ dimer dissociated to Mo single atoms on Rh(111).
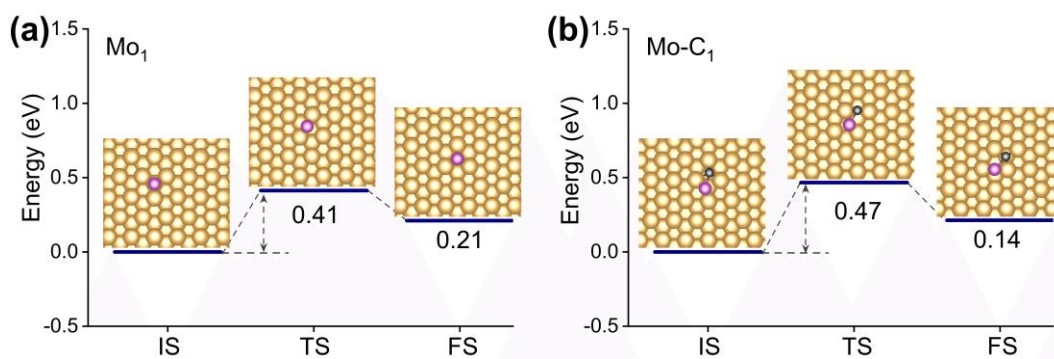
Fig. S5. Diffusion E_{bar} for Mo single atom and Mo-C_1 species from the most stable to metastable site of Rh(111) substrate.
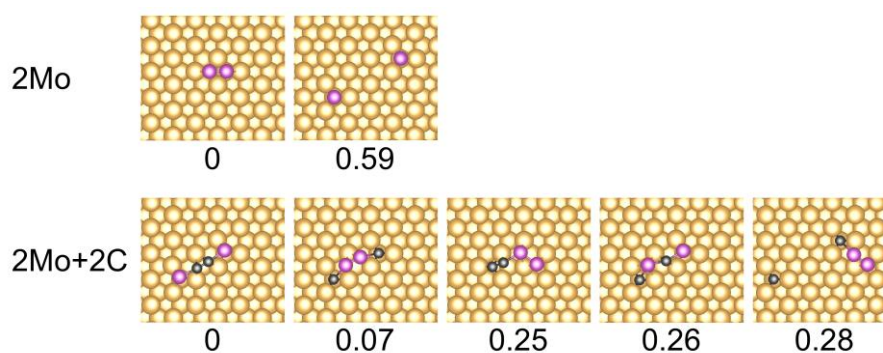
Fig. S6. Configurations and relative energies of two Mo atoms without/with the introduction of C atoms on Rh(111).
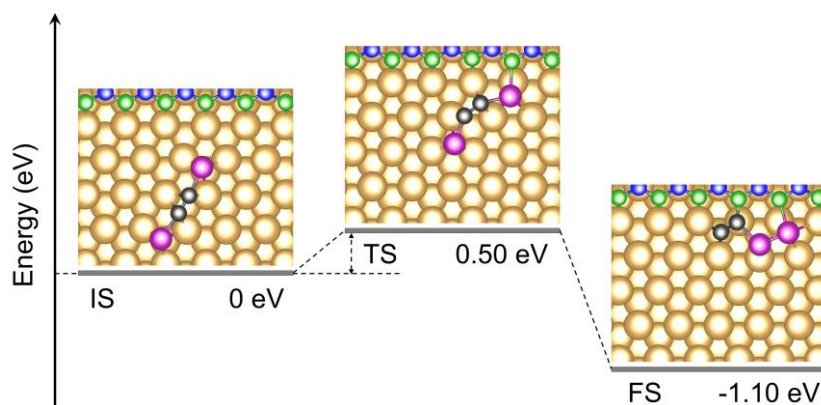
Fig. S7. The MEP and E_{bar} for Mo-C_2-Mo species migrating to the hBN edge on Rh(111) during the initial nucleation stage.
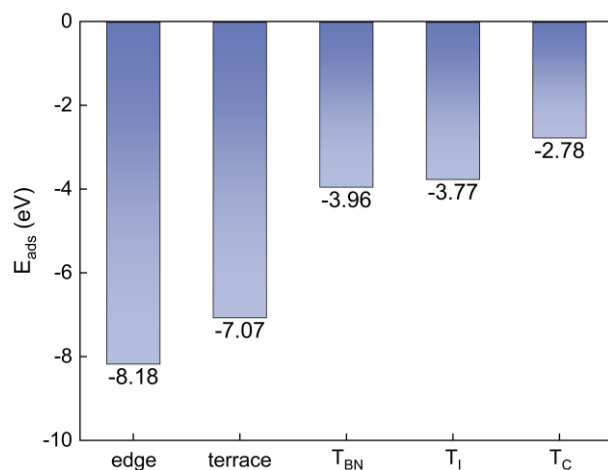
Fig. S8. The optimized adsorption energy (E_{ads}) for a C_2 dimer adsorption on the edge, terrace, T_{BN}, T_I, and T_C of h-BN-G lateral heterostructure on Rh(111).

We have further investigated the adsorptions of a C_2 dimer on the edge sites and terrace surfaces of h-BN-G lateral heterostructures grown on Rh(111), as well as on three top surfaces of the synthesized 2D lateral heterostructures: the top of BN (T_{BN}), graphene (T_C), and interface (T_I). The E_{ads} of the C_2 dimer is calculated using the following equation:

$$E_{ads}(C_2) = E(C_2/hBNG/Rh(111)) - E(hBNG/Rh(111)) - E(C_2), \qquad (3)$$

In this equation, the three terms on the right side represent the total energy of the C_2 dimer adsorbing on h-BN-G lateral heterostructures on Rh(111), h-BN-G/Rh(111) complex, C_2 dimer in the gas phase, respectively.

Tab. S1. Calculated relative energies (in eV) for separation and/or dimerization of B and N atoms without/with TM-SAC on Rh(111). For the cases with TM-SAC (TM=Mo, Mn, Zr, Nb, Hf, Ta, and W), there is two linking types of TM-N and TM-B couplings, and the dimerization of TM-NB (TM-N coupling) is set as a reference value.

	Separation	Dimerization	ΔE
Without TM	0.18	0	0.18
Mo-N	1.11	0	1.11
Mo-B	1.19	1.15	0.04
Mn-N	0.80	0	0.80
Mn-B	0.69	0.40	0.29
Zr-N	1.18	0	1.18
Zr-B	1.12	1.07	0.05
Nb-N	1.32	0	1.32
Nb-B	1.21	1.17	0.04
Hf-N	1.21	0	1.21
Hf-B	1.11	1.05	0.06
Ta-N	1.41	0	1.41
Ta-B	1.28	1.27	0.01
W-N	1.46	0	1.46
W-B	1.36	1.26	0.10
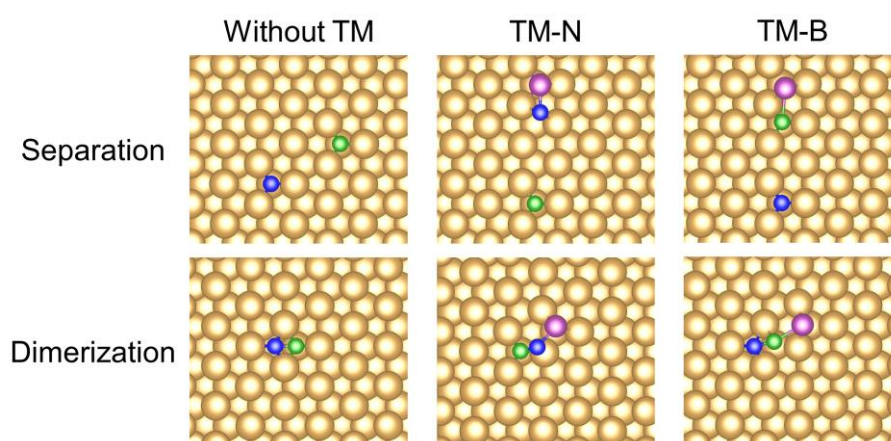
Fig. S9. Configurations of separation and dimerization of the B and N atoms without/with TM-SAC on Rh(111).
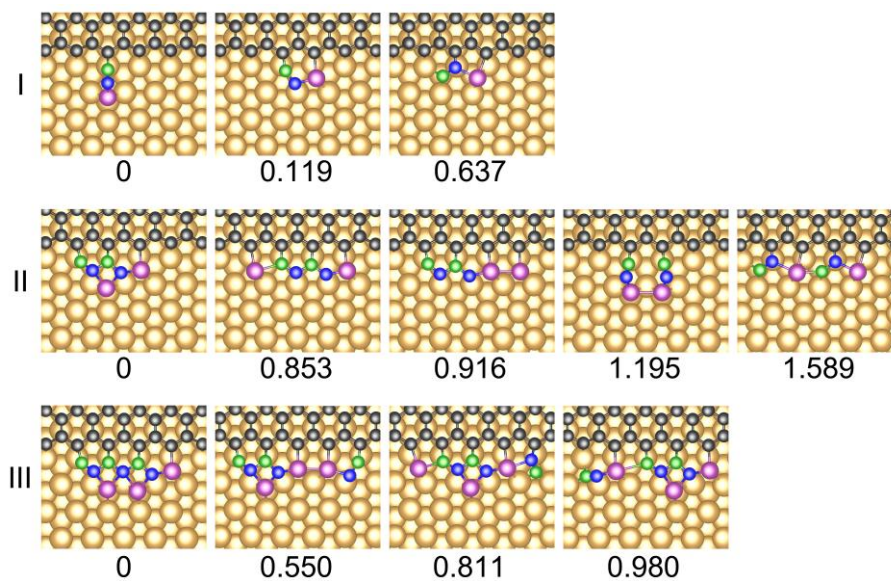
Fig. S10. Configurations and relative energies of the growth of BN-Mo seeds attaching to the graphene edge on Rh(111).

Fig. S11. Calculated MEP for the initial nucleation stage in forming 1D *h*-BN-G. Here, BN-Mo serves as the feeding block attaching to the zigzag C edge of graphene domain. The E_{bar} for the key steps (from TS_1 to TS_3) is shown in the illustration.

Fig. S12. The free energy diagram for hydrogen evolution reaction (HER) at the interfacial C atom of C-B and C-N interface, graphene domain, and h-BN domain of 1D h-BN-G heterostructure.
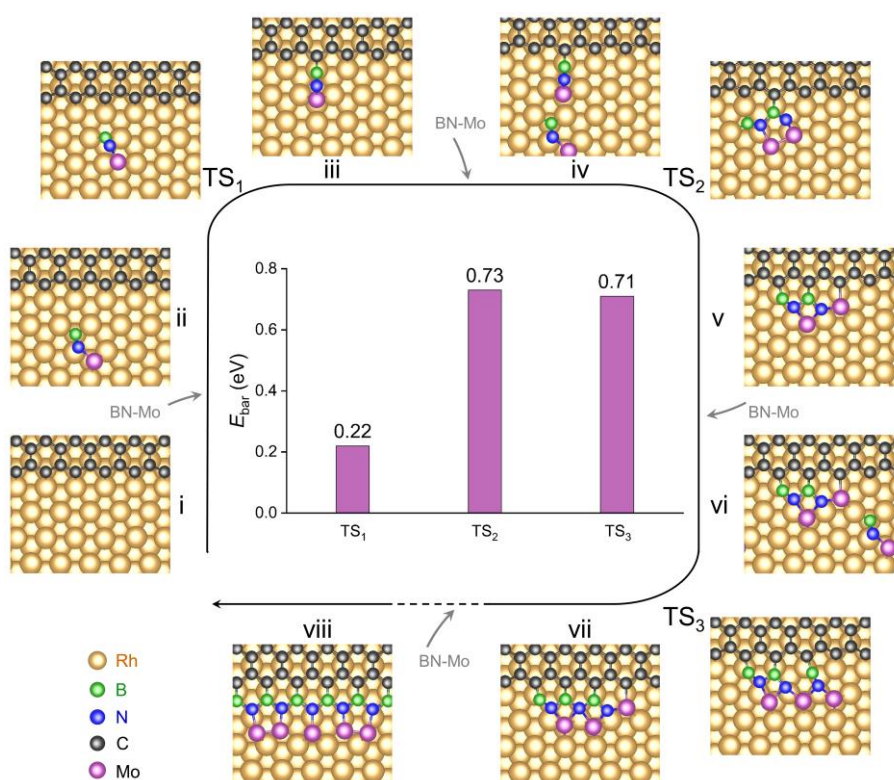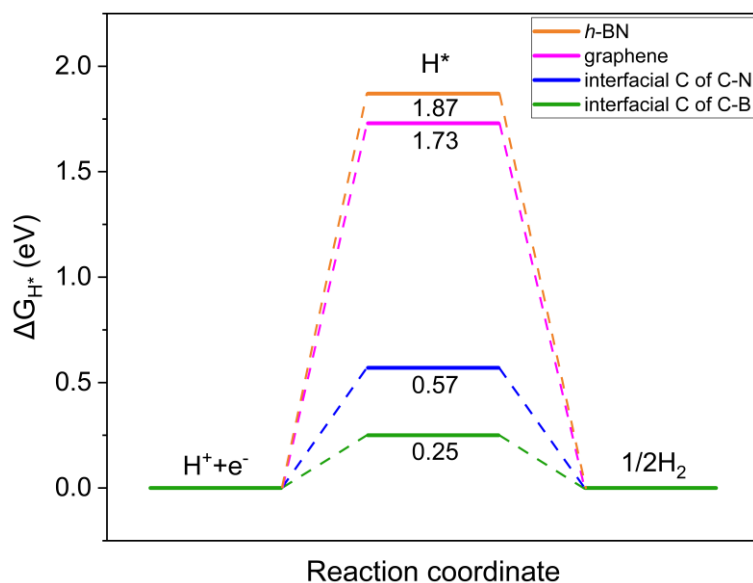
Taking hydrogen evolution reaction (HER) as a typical example, we have further briefly examined the potential catalytic performance of h-BN-G lateral heterostructure. First, we calculate the hydrogen adsorption energy (ΔE_H) on high-symmetry sites of a free-standing h-BN-G heterostructure, with a definition as:

$$\Delta E_H = E(hBNG+H^*) - E(hBNG) - 1/2E(H_2), \qquad (4)$$

where $E(hBNG+H^*)$ is the total energy of h-BN-G lateral heterostructure with hydrogen adsorption, $E(hBNG)$ is the energy of a clean h-BN-G, and $E(H_2)$ is the energy of the H_2 molecule in the gas phase. Negative values indicate exothermic reactions. Hydrogen adsorption at the interfacial C atom of the C-B and C-N interfaces yields lower ΔE_H values, with exothermic energies of 0.32 and 0.06 eV, respectively. In contrast, hydrogen adsorption on graphene and h-BN is unfavorable, with endothermic energies of 1.15 and 1.24 eV, respectively.

Moreover, the calculated Gibbs free energies for HER process occur at the interfacial C atom of C-B and C-N interface, graphene domain, and h-BN domain are 0.25 and 0.57, 1.73, and 1.87 eV, with the former being closer to zero, see Fig. S12. Note also that, as emphasized in the main text, the introduction of Mo-SAC preferentially leads to the C-B-linked h-BN-G heterostructure, which significantly enhances hydrogen adsorption and potentially offering catalytic performance similar to that of metal anchored B_5N_3 catalysts.[1] These findings imply that, with the aids of TM-SACs, the formed C-B-linked h-BN-G heterostructure may exhibit high-performance catalysis for HER.

Here, we include the Gibbs free energy for hydrogen adsorption calculated by taking zero point energy and entropy corrections into account such that:[2]

$$\Delta G_{H*} = \Delta E_H + \Delta E_{ZPE} - T\Delta S, \tag{5}$$

where ΔE_{ZPE} and ΔS are the difference in zero point energy and entropy between the adsorbed hydrogen and hydrogen in the gas phase, and T is the temperature. Since the vibrational entropy of H^* in the adsorption state is small, the entropy of adsorption of $1/2H_2$ is $\Delta S_H \approx -1/2S_{H2}^0$, where S_{H2}^0 is the entropy of H_2 in the gas phase at standard conditions.
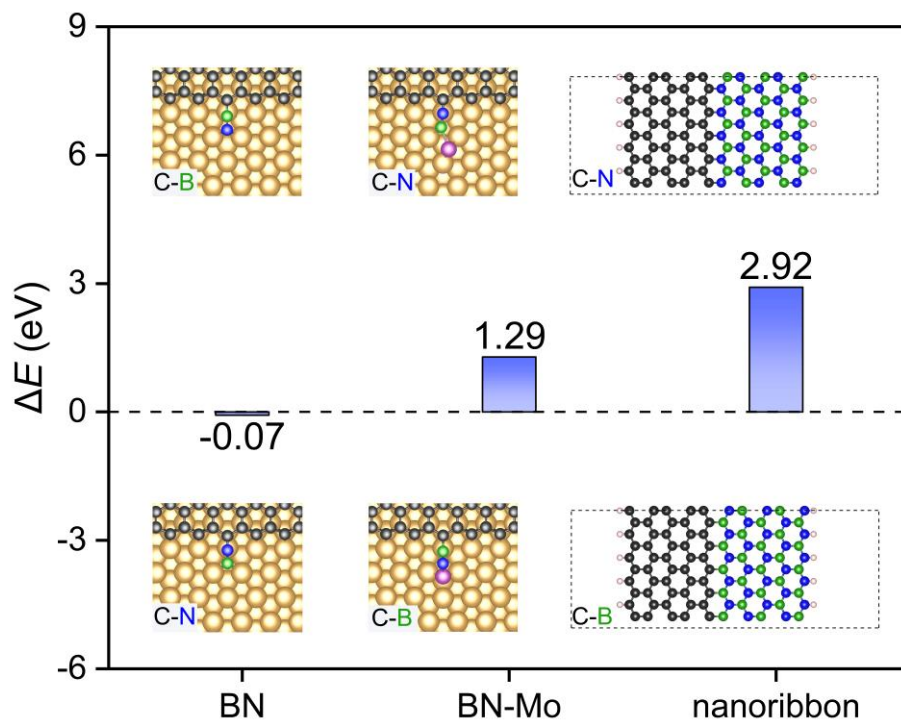
Fig. S13. Calculated ΔE between two types of boundary linking of C-N and C-B for the process of a BN dimer attaching to C edge on Rh(111) without/with Mo-SAC with the definition:

$$\Delta E = E_{C\text{-}N} - E_{C\text{-}B}, \qquad (6)$$

where the two terms of $E_{C\text{-}N}$ and $E_{C\text{-}B}$ represent the optimized energies of the two types of linking boundaries of C-N and C-B, respectively. Note that, the three structures inserted in the bottom panels are 0.07, 1.29, and 2.92 eV lower in energies than their top-panel counterparts, respectively.
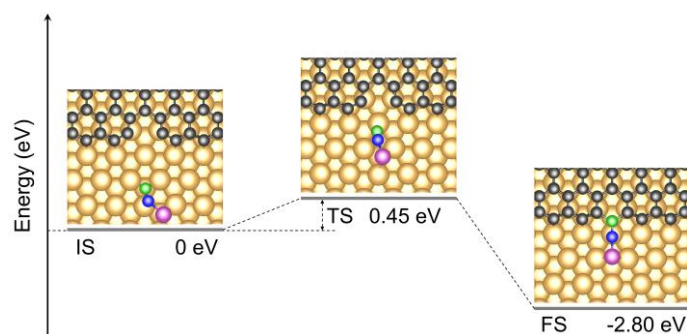
Fig. S14. The MEP and E_{bar} for BN-Mo species migrating to the C-vacancy of the graphene edge on Rh(111) during the initial nucleation stage.
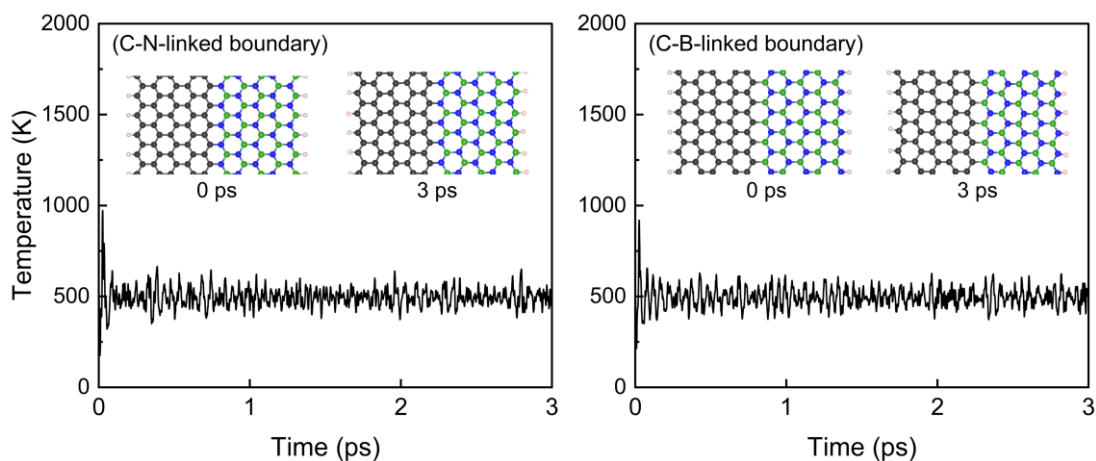

Fig. S15. AIMD simulation. The thermodynamic properties of two typical free-standing 1D *h*-BN-G heterostructures, with (a) C-N- and (b) C-B-linked boundaries, are presented along with representative snapshots of their initial and final geometric structures as functions of AIMD simulation time at 500 K, with a time step of 1 fs.

References

1. Y. Zhang, Z. Zeng and H. Li, *J. Mater. Chem. A*, 2022, **10**, 9737-9745.
2. J. K. Nørskov, T. Bligaard, A. Logadottir, J. R. Kitchin, J. G. Chen, S. Pandelov and U. Stimming, *J. Electrochem. Soc.*, 2005, **152**, J23-J26.